Incorporation of Water into Glasses and its Influence on the Diffusion of Cations, Including the Creation of Diffusion Barriers
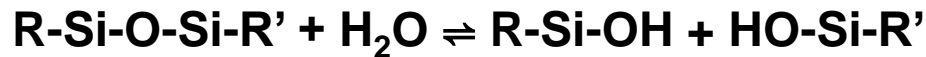
Rüdiger Dieckmann

Department of Materials Science and Engineering, Bard Hall, Cornell University, Ithaca, NY 14853-1501

Water in Silicate Glasses I

- **how is water accommodated?**
  - most in the form of OH groups, little in the form of water molecules
  - OH groups are formed by reaction between water molecules and the glass network by the reaction

    R-Si-O-Si-R' + H_2O $\rightleftharpoons$ R-Si-OH + HO-Si-R'

- **how much water can be accommodated in glasses?**
  - depends on several parameters:
    - purity of the raw materials used for making the glass
    - chemical composition of the glass
    - thermal history of the glass
    - annealing conditions, i.e., temperature, total pressure, water vapor pressure
    - sample geometry
    - time of annealing
  - sample may or may not be completely equilibrated during annealing, the latter leading to a non-uniform water distribution
  - very large water contents are possible

Water in Silicate Glasses II

- **processes involved in the incorporation of water into glass?**
  - transport of H_2O molecules within the surrounding atmosphere to the gas/glass interface; occurs usually very fast and has therefore in most cases no influence on the overall reaction rate
  - reaction at the gas/glass interface, e.g., $H_2O_{(gas)} \rightleftharpoons H_2O_{(glass)}$
  - transformation of H_2O into OH groups within the glass, i.e., the reaction R-Si-O-Si-R' + H_2O $\rightleftharpoons$ R-Si-OH + HO-Si-R'
  - transport within the glass, i.e., diffusion of H_2O molecules and of OH groups; usually the diffusion of H_2O molecules is much faster than that of OH groups
- **kinetics of water uptake during annealing at high temperatures?**
  - depend on the rates of the reactions denoted above and on the diffusivities of water-related species in the glass
  - limiting cases: diffusion control and reaction control

How to Measure the Water Content of Glasses?

- $c_{OH} \gg c_{H_2O}$; therefore measure only c_{OH}

- IR absorption due to OH stretching vibration at a wavenumber of about 3600 cm^{-1}

- intensity of this absorption is related to the concentration of OH and to the overall water concentration

- absorption due to OH groups is described by the Beer-Lambert law:

$$I \approx I_0 \cdot e^{-\alpha_{OH} \cdot c_{OH}^m \cdot \ell_g}$$

$$I \approx I_0 \cdot 10^{-\varepsilon_{OH} \cdot c_{OH}^m \cdot \ell_g} = I_0 \cdot 10^{-A_g}$$

- relation between the absorbance A_g and the concentration of OH groups:

○ ε_{OH} = molar absorption coefficient related to the overall concentration of OH groups present in the glass ($\ell/(mol_{OH} \cdot cm)$)

○ ℓ_g = thickness of glass sample (cm)

○ c_{OH}^m = molar concentration of OH

○ A_g = absorbance

○ c_{OH}, c_{H_2O} = mass fractions of OH, H_2O

○ M_{OH}, M_{H_2O} = molar masses of OH, H_2O

○ ρ_g = density of the glass (g/cm^3)

○ I/I_0 = ratio between transmitted and initial IR signal

○ ε_{H_2O} = molar absorption coefficient related to the overall concentration of H_2O in the glass ($\ell/(mol_{H_2O} \cdot cm) = 2\,\varepsilon_{OH}$

$$A_g = -\log \frac{I}{I_0} = c_{OH} \cdot \varepsilon_{OH} \cdot \ell_g \cdot \frac{\rho_g}{M_{OH}} = 2\,c_{H_2O} \cdot \varepsilon_{OH} \cdot \ell_g \cdot \frac{\rho_g}{M_{H_2O}} = c_{H_2O} \cdot \varepsilon_{H_2O} \cdot \ell_g \cdot \frac{\rho_g}{M_{H_2O}}$$

FTIR Measurement of the OH-Content of Glasses

- **from the Beer-Lambert law:**

$$c_{H_2O} = \frac{M_{H_2O}}{m_{glass}} = \frac{1}{2} \cdot \frac{A_g}{\varepsilon_{OH} \cdot \ell_g} \cdot \frac{M_{H_2O}}{\rho_g}$$

with

$$A_g = -\log_{10}\left(\frac{I}{I_0}\right)$$

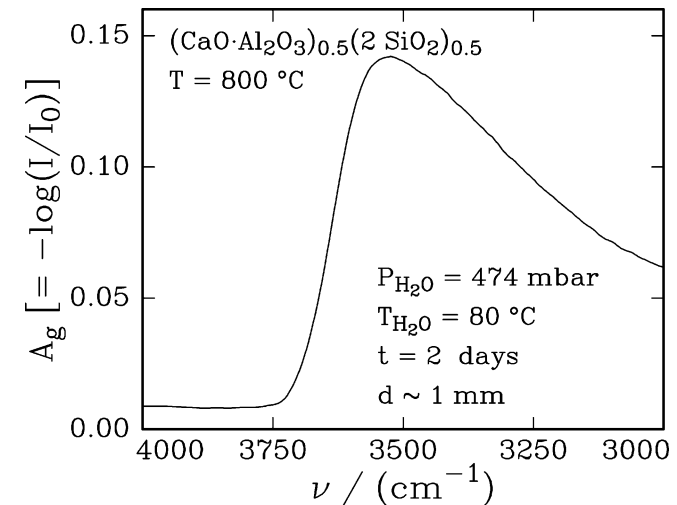- **reorganization of the equation for c_{H_2O}:**

$$c_{H_2O} \cdot \varepsilon_{OH} = \frac{1}{2} \cdot \frac{A_g}{\ell_g} \cdot \frac{M_{H_2O}}{\rho_g}$$

- **change in the H_2O concentration after annealing for the time t:**

$$\Delta c_{H_2O} = c_{H_2O}(t) - c_{H_2O}(t = 0)$$

$(CaO \cdot Al_2O_3)_{0.5}(2\ SiO_2)_{0.5}$
T = 800 °C
$P_{H_2O} = 474$ mbar
$T_{H_2O} = 80$ °C
t = 2 days
d ~ 1 mm

- ε_{OH} = molar absorption coefficient related to the overall concentration of OH groups present in the glass ($\ell/(mol_{OH} \cdot cm)$)
- ℓ_g = thickness of glass sample (cm)
- c_{H_2O} = mass fraction of H_2O
- M_{H_2O} = molar mass of H_2O (= 18 g/mol)
- ρ_g = density of the glass (g/cm³)
- I/I_0 = ratio between transmitted and initial IR signal

Structural Changes Upon the Uptake of Water — Structural Relaxation

- **structural changes due to the uptake of water:**
  - water molecules accommodated as such may cause local changes in the spacing between glass components
  - the formation of OH-groups by the reaction R-Si-O-Si-R' + H_2O ⇌ R−Si−OH + HO−Si−R' may also lead to local structural changes
  - more important: the dynamical nature of the equilibrium reaction denoted above
    - temporary formation of OH-groups and subsequent formation of H_2O molecules enables the glass network to undergo a structural relaxation
    - long range structural changes can take place, leading to changes in bonding angles and distances
    - for silica glass experimentally confirmed by Tomozawa and his group that such structural changes occur

- **expectation:**
  all structure-sensitive properties of glasses (e.g., viscosities, diffusivities, etc.) change when structural changes occur due a water uptake

Opportunity for Generating Functionally Graded Glass?

- **if the uptake of water leads to useful property changes, water incorporation can be used to generate glass with properties changing as a function of the distance from the surface**
  - **low tech approach**
  - **low cost**

- **by annealing glass in a moist atmosphere at high temperature the properties of the near-surface region may be changed while the rest of the glass remains unchanged**

- **example of interest here:**
  - **modification of the diffusivity of ions by the incorporation of water**
  - **can be used to generate a diffusion barrier if the diffusivity of interest in the water uptake-influenced region is significantly smaller than in the rest of the sample**

Silicate Glasses of Interest

- **Type I silica (Heraeus Infrasil 302)**
  - **fused quartz made by melting of natural quartz crystals**
  - **average concentration of metallic impurities: about 40 ppm by weight**
    - **most abundant: Al (about 30 ppmw)**
    - **Ti, Fe and Na present at the one ppmw level**
    - **OH content less than 8 ppmw**
  - **strain point: 1075 °C**

- **Corning Code 1737 glass**
  - **alkaline earth boroaluminosilicate glass**
  - **composition (in mol %): SiO_2 69.0 %, Al_2O_3 11.5 %, B_2O_3 7.3 % CaO 5.0 %, BaO 4.4 %, MgO 1.4 %, SrO 1.2 % and As_2O_3 0.2 %, Na impurity level 600 ppma; OH about 500 ppmw**
  - **fusion drawn substrate glass for flat panel display applications**
  - **strain point 666 °C**

- **model glasses of the type $(CaO \cdot Al_2O_3)_{1-x}(2\ SiO_2)_x$**

Topics of Interest

- **questions:**
  - ○ how fast is water taken up?
  - ○ which type of kinetics determines the water uptake?
  - ○ how large are the diffusion rates of sodium cations in general?
  - ○ how are these rates influenced by water taken up during pre-annealing and/or during diffusion annealing?
  - ○ can the uptake of water by a glass produce something useful, e.g., be used to generate barrier layers?
  - ○ if yes, how effective are such barrier layers?
- **experiments:**
  - ○ infrared absorption studies on the integral rate of the water uptake
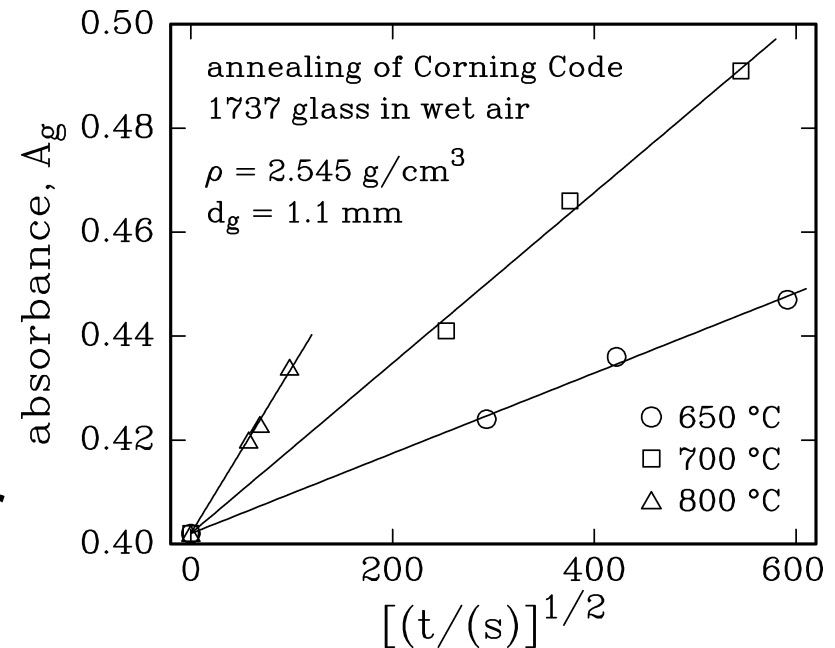 - ○ tracer diffusion experiments with Na-22

Water Uptake by Corning Code 1737 Glass I

- **experiments:**
  - ○ **annealing of glass samples for different times in wet air (air saturated with water at 80 °C) at 650, 700 and 800 °C**
  - ○ **measurement of the absorbance related to OH groups**

- **results:**
  - ○ **analysis of the time dependence of the absorbance shows that it increases with the square root of the annealing time**
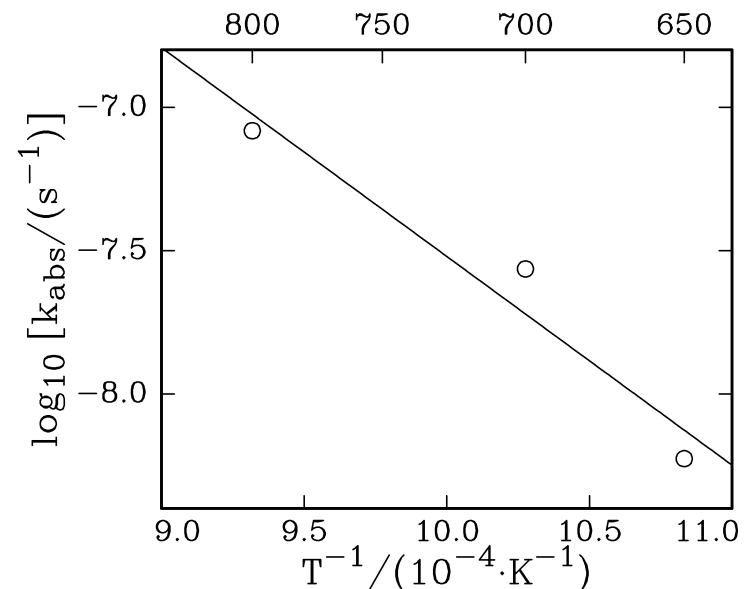 - ○ **indicates that the uptake of water is a diffusion-controlled process**

annealing of Corning Code 1737 glass in wet air

$\rho = 2.545 \text{ g/cm}^3$
$d_g = 1.1 \text{ mm}$

○ 650 °C
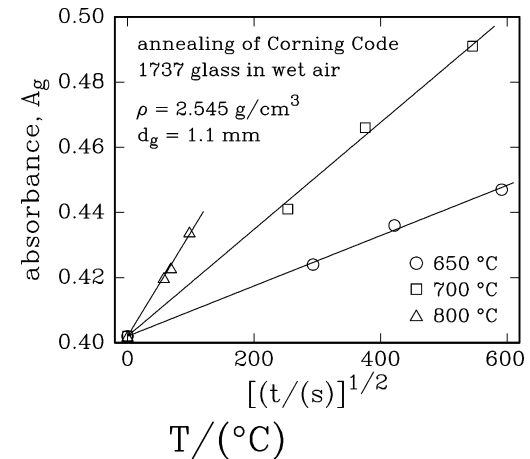□ 700 °C
△ 800 °C

absorbance, A_g

$[(t/(s)]^{1/2}$

Water Uptake by Corning Code 1737 Glass II

- ## water content:
  - absorbance observed at t = 0 corresponds to an OH concentration of about 500 ppm by weight
  - estimated that the OH concentrations at the glass surface could be about 20 times higher at 650, 700 and 800 °C in wet air

- ## kinetics:
  - time dependence of absorbance: $A_g(t) = A_g(t=0) + (k_{abs} \cdot t)^{1/2}$
  - k_{abs} obtained from the slopes in the plot shown before
  - T-dependence of k_{abs}: activation energy = 139.5 ($\pm$ 34.5) kJ/mol; to be attributed to the diffusion of H_2O
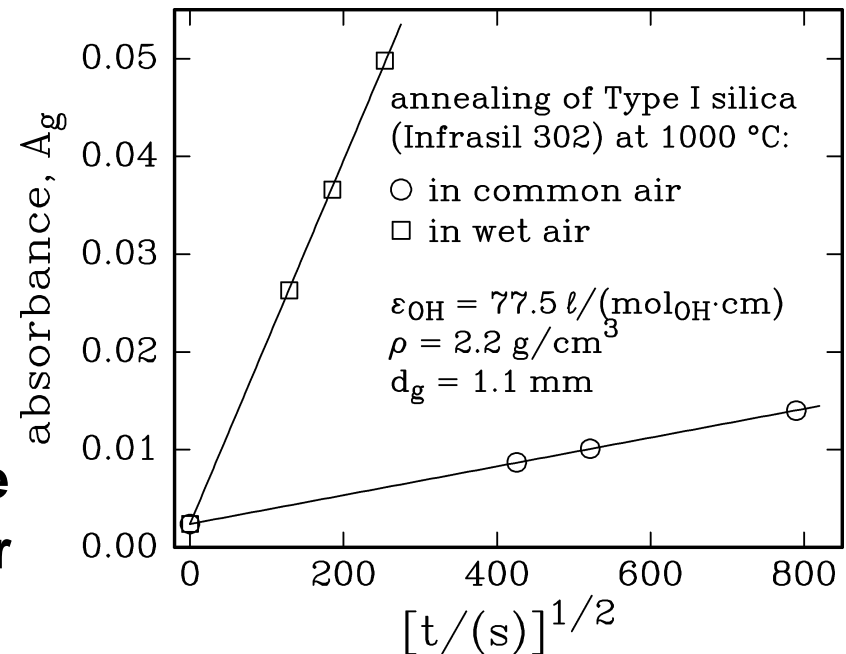

annealing of Corning Code 1737 glass in wet air

ρ = 2.545 g/cm^3
d_g = 1.1 mm

○ 650 °C
□ 700 °C
△ 800 °C

Water Uptake by Type I Silica Glass (Infrasil 302) I

- **experiments:**
  - ○ **annealing of glass samples for different times in wet and common air (air saturated with water at 80 °C) at 1000 °C**
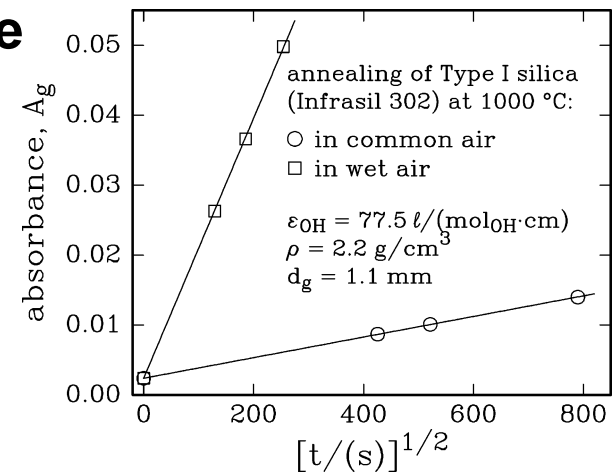 - ○ **measurement of the absorbance related to OH groups**

- **results:**
  - ○ **analysis of the time dependence of the measured absorbance shows that the absorbance increases as function of the square root of the annealing time**
  - ○ **indicates that the uptake of water is a diffusion-controlled process**

annealing of Type I silica (Infrasil 302) at 1000 °C:

○ in common air
□ in wet air

$\varepsilon_{OH} = 77.5\,\ell/(mol_{OH}\cdot cm)$
$\rho = 2.2\ g/cm^3$
$d_g = 1.1\ mm$

absorbance, A_g

$[t/(s)]^{1/2}$

Water Uptake by Type I Silica Glass (Infrasil 302) II

- **water content:**
  - absorbance observed at t = 0 corresponds to an OH concentration of about 2 ppm by weight
  - estimated that the OH concentrations at the glass surface could be about 160 and 800 ppm by weight in common and in wet air, respectively
  - OH concentration ratio is in good agreement with that expected based on equilibrium water pressures at 18 and 80 °C

annealing of Type I silica (Infrasil 302) at 1000 °C:
○ in common air
□ in wet air

$\varepsilon_{OH} = 77.5 \; \ell/(mol_{OH} \cdot cm)$
$\rho = 2.2 \; g/cm^3$
$d_g = 1.1 \; mm$

(plot axes: absorbance, A_g versus $[t/(s)]^{1/2}$)

- **kinetics:**
  - time dependence of the absorbance: $A_g(t) = A_g(t=0) + (k_{abs} \cdot t)^{1/2}$
  - values for k_{abs} obtained from the slopes in the plot shown before
  - k_{abs}(wet air)/k_{abs}(common air) ≈ 160, i.e., much larger than the corresponding P_{H_2O}-ratio; the reason for this is unknown
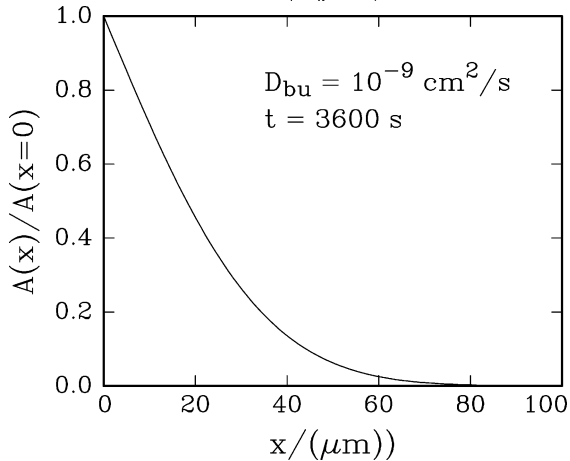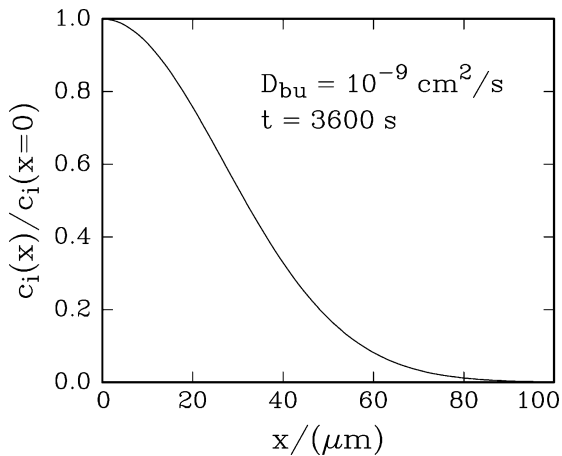
Sodium Diffusion Profiles I

- **radioactive tracer (Na-22) always applied as a thin film**

- **in all diffusion experiments residual radioactivity profiles measured**

- **after diffusion annealing, residual radioactivity profiles determined, i.e., residual radioactivity measured after the successive removal of sample material beginning at the surface where tracer was applied**

- **different types of concentration profiles observed after diffusion-annealing, different solutions of Fick's 2nd law apply for $c_i(x,t)$ (i = Na-22)**

- **residual radioactivity after removal of material of the thickness x:**

$$\frac{A(x)}{A(x=0)} = \frac{\int_{x}^{\infty} c(x) \cdot dx}{\int_{0}^{\infty} c(x) \cdot dx} = f(x,t)$$
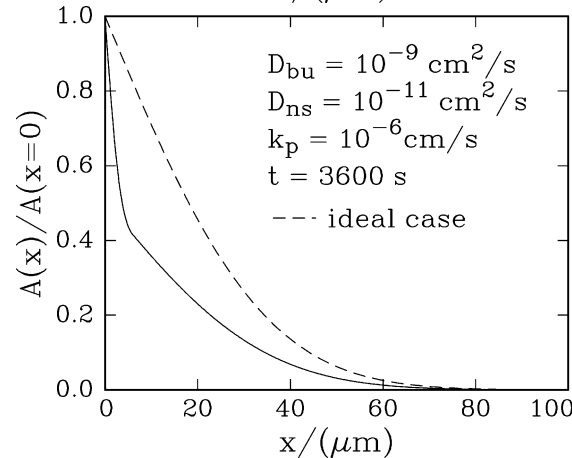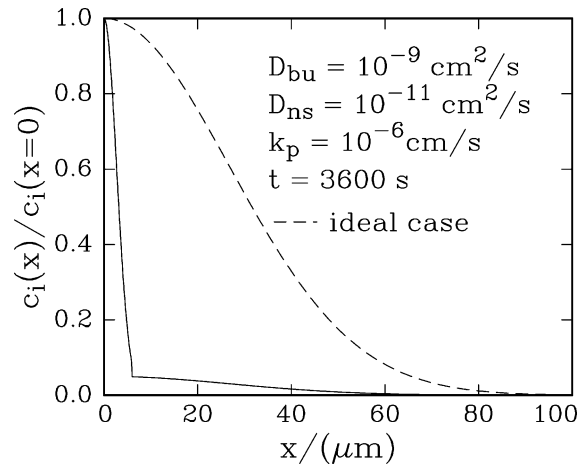
- **in the following, discussion of different cases of relevance**
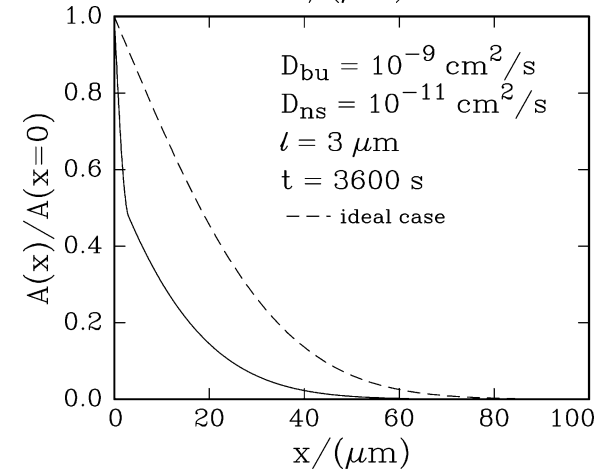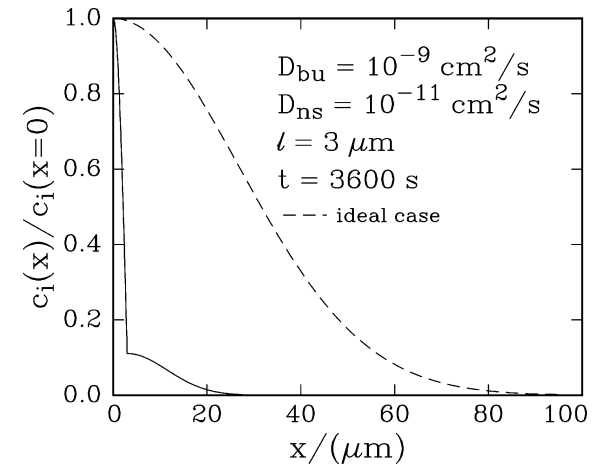
Sodium Diffusion Profiles II

● **profiles for Case A:**   ● **profiles for Case B:**   ● **profiles for Case C:**

Sodium Diffusion Profiles III

- **if the samples are homogeneous with regard to their chemical composition and their structure, the thin film solution of Fick's 2nd law applies**

$$c_i(x,t) = \frac{Q_i}{\sqrt{\pi \cdot D_i \cdot t}} \cdot \exp\left(-\frac{x^2}{4\,D_i \cdot t}\right)$$

- **residual radioactivity after removal of material of the thickness x:**

$$\frac{A(x)}{A(x=0)} = \frac{\int\limits_{x}^{\infty} c(x) \cdot dx}{\int\limits_{0}^{\infty} c(x) \cdot dx} = 1 - \text{erf}\left(\frac{x}{2\sqrt{D_i \cdot t}}\right)$$

- **in the following, this case will be denoted as Case A**

Sodium Diffusion Profiles IV

- **if the samples are inhomogeneous, different solutions of Fick's 2nd law need to be applied**

- **considered are samples with a near-surface region, in which the diffusion rate is different from that in the bulk, i.e., $D_i(ns) \neq D_i(bu)$**

- **two cases of interest:**
  - **Case B: thickness of the near-surface region, ℓ, changes with the diffusion-annealing time, $\ell = (k_{p(da)} \cdot t_{da})^{1/2}$**
  - **Case C: thickness of the near-surface region, ℓ, does not change with the diffusion-annealing time (but with the time of pre-annealing at a significantly higher temperature than that of the diffusion anneal, i.e., $\ell = (k_{p(pa)} \cdot t_{pa})^{1/2}$)**

- **different solutions for $x < \ell$ and for $x > \ell$**

ℓ

surface | near-surface region | bulk region

$D_i(ns)$ | $D_i(bu)$

x
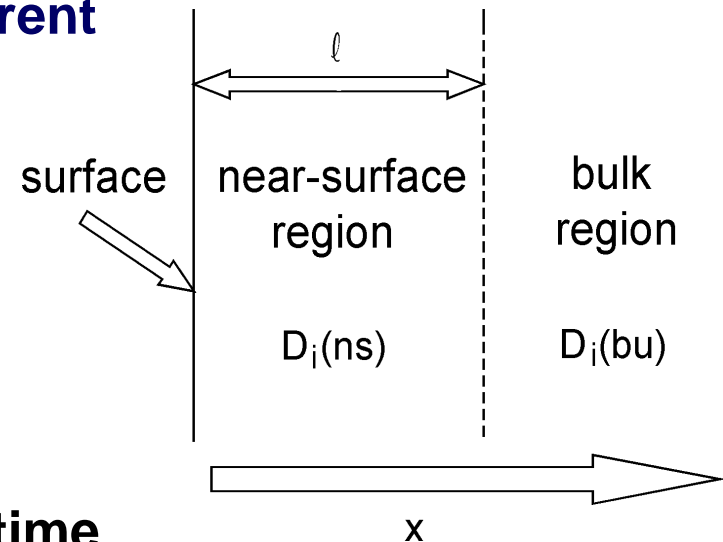
Sodium Diffusion Profiles V

- **solution for Case B:**
  - **for x < ℓ:**

$$\frac{A(x < \ell)}{A(x = 0)} = 1 - \frac{\mathrm{erf}\left(\dfrac{x}{2\sqrt{D_{ns} \cdot t}}\right)}{\mathrm{erf}\left(\dfrac{1}{2}\sqrt{\dfrac{k_{p(da)}}{D_{ns}}}\right) + \sqrt{\dfrac{D_{bu}}{D_{ns}}} \cdot \exp\left(\dfrac{k_{p(da)}}{4D_{bu}} - \dfrac{k_{p(da)}}{4D_{ns}}\right) \cdot \mathrm{erfc}\left(\dfrac{1}{2}\sqrt{\dfrac{k_{p(da)}}{D_{bu}}}\right)}$$

  - **for x > ℓ:**

$$\frac{A(x > \ell)}{A(x = 0)} = \frac{\mathrm{erfc}\left(\dfrac{x}{2 \cdot \sqrt{D_{bu} \cdot t}}\right)}{\mathrm{erfc}\left(\dfrac{1}{2}\sqrt{\dfrac{k_{p(da)}}{D_{bu}}}\right) + \sqrt{\dfrac{D_{ns}}{D_{bu}}} \cdot \exp\left(\dfrac{k_{p(da)}}{4D_{ns}} - \dfrac{k_{p(da)}}{4D_{bu}}\right) \cdot \mathrm{erf}\left(\dfrac{1}{2} \cdot \sqrt{\dfrac{k_{p(da)}}{D_{ns}}}\right)}$$

- **solution for Case C:**
  - **for x < ℓ:**

$$\frac{A(x < \ell)}{A(x = 0)} = \mathrm{erf}\left[\frac{x}{2\sqrt{D_{Na}^*(ns) \cdot t}}\right] \cdot \sum_{n=0}^{\infty} \lambda^{n+1} \cdot \left(\mathrm{erf}\left[\frac{(2n+2)\cdot \ell + x}{2\sqrt{D_{Na}^*(ns) \cdot t}}\right] - \mathrm{erf}\left[\frac{(2n+2)\cdot \ell - x}{2\sqrt{D_{Na}^*(ns) \cdot t}}\right]\right)$$
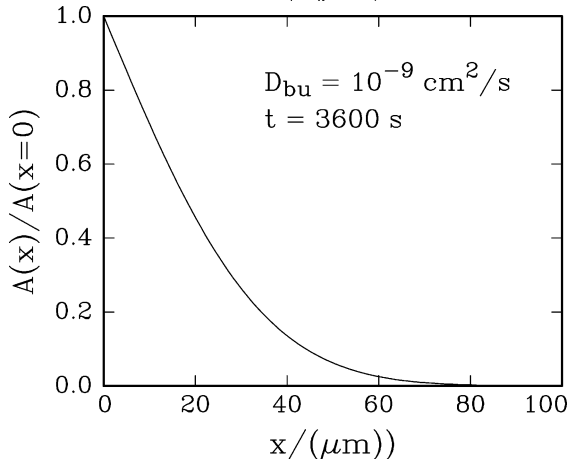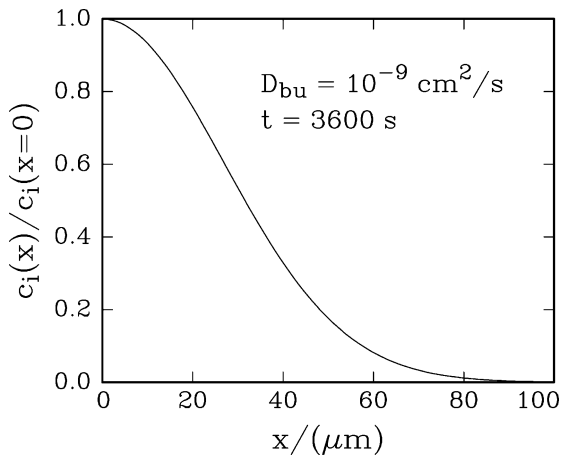
  - **for x > ℓ:**

$$\frac{A(x > \ell)}{A(x = 0)} = \frac{2\alpha}{\alpha + 1} \cdot \sum_{n=0}^{\infty} \lambda^n \cdot \mathrm{erfc}\left[\frac{(2n+1)\cdot \ell + \alpha^{-1} \cdot (x - \ell)}{2\sqrt{D_{Na}^*(ns) \cdot t}}\right]$$

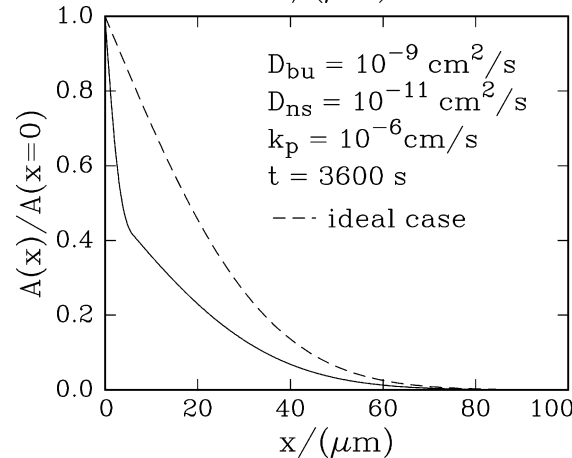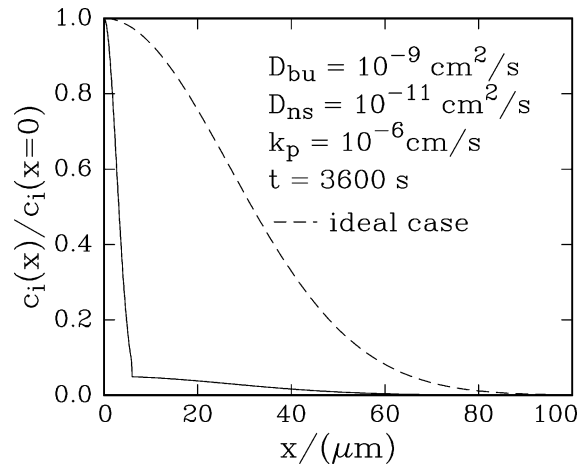**where** $\quad \alpha = \sqrt{\dfrac{D_{Na}^*(bu)}{D_{Na}^*(ns)}} \quad$ **and** $\quad \lambda = \dfrac{1 - \alpha}{1 + \alpha}$
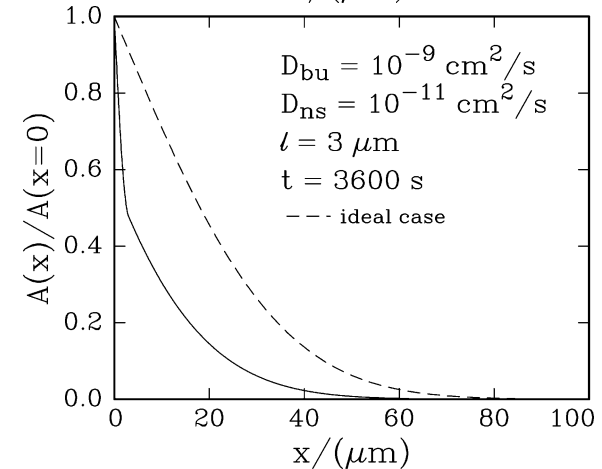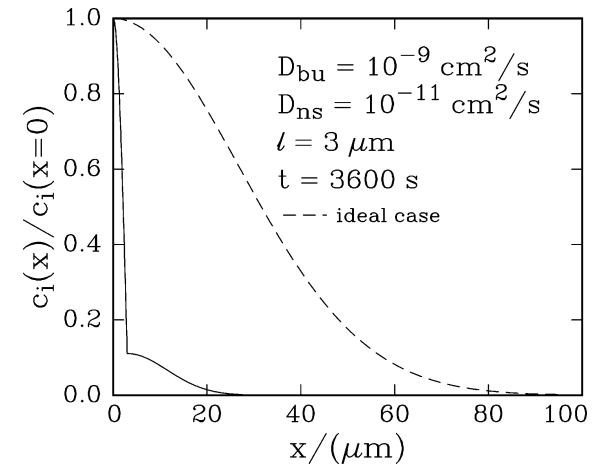
Sodium Diffusion Profiles VI
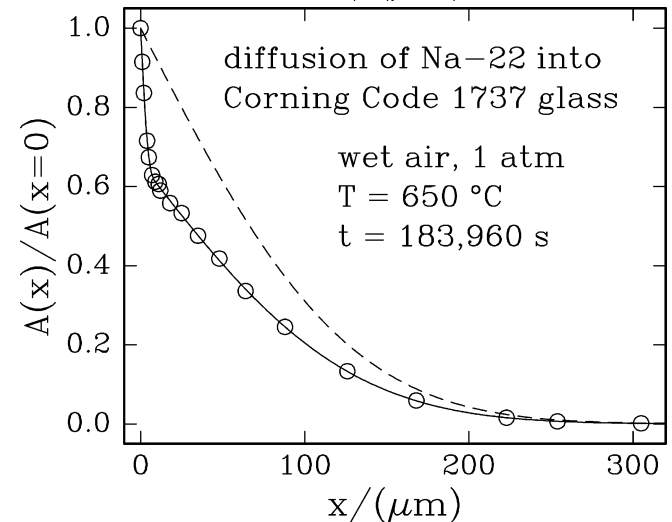
- **profiles for Case A:**
- **profiles for Case B:**
- **profiles for Case C:**

$D_{bu} = 10^{-9}$ cm^2/s
t = 3600 s

$D_{bu} = 10^{-9}$ cm^2/s
$D_{ns} = 10^{-11}$ cm^2/s
$k_p = 10^{-6}$ cm/s
t = 3600 s
--- ideal case

$D_{bu} = 10^{-9}$ cm^2/s
$D_{ns} = 10^{-11}$ cm^2/s
$\ell = 3\ \mu$m
t = 3600 s
--- ideal case

$D_{bu} = 10^{-9}$ cm^2/s
t = 3600 s

$D_{bu} = 10^{-9}$ cm^2/s
$D_{ns} = 10^{-11}$ cm^2/s
$k_p = 10^{-6}$ cm/s
t = 3600 s
--- ideal case

$D_{bu} = 10^{-9}$ cm^2/s
$D_{ns} = 10^{-11}$ cm^2/s
$\ell = 3\ \mu$m
t = 3600 s
--- ideal case
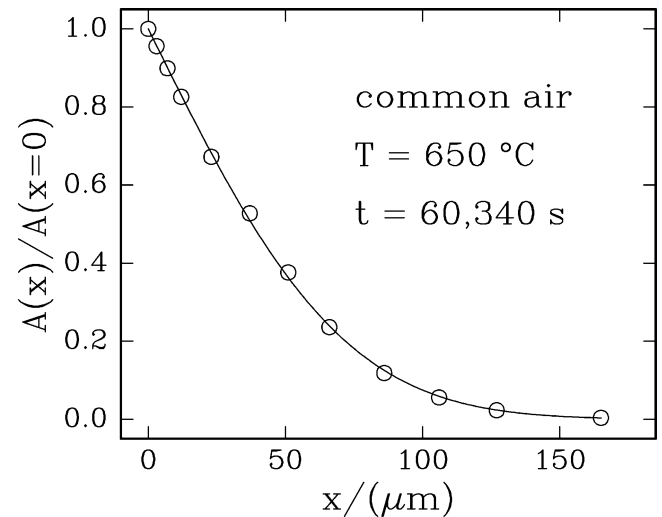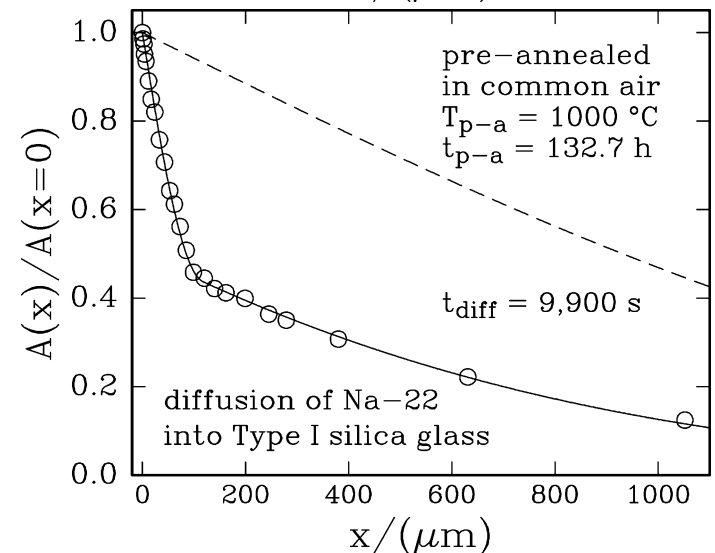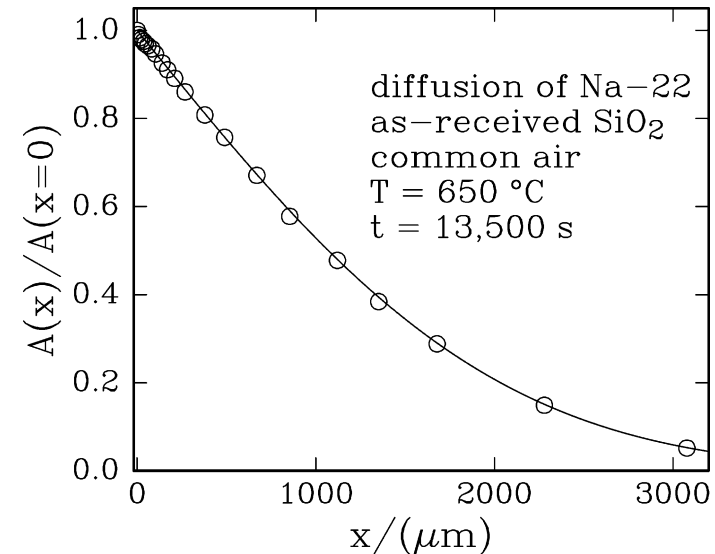
Diffusion of Na in 1737 Glass I

- **diffusion-annealing of as-received samples in dry and in common air leads to type A profiles, i.e., to profiles that can be described by a single diffusion coefficient**

- **type B profiles with kinks are observed after diffusion-annealing of as-received samples in wet air (i.e., air saturated with H$_2$O at 80 °C)**

- **the location of the kink changes with the diffusion-annealing time**

- **the kink displacement with the diffusion-annealing time follows a parabolic rate law, as assumed for type B profiles**

- **the presence of sharp kinks justifies the assumption that D$_{Na}$(ns) is constant**

common air
T = 650 °C
t = 60,340 s

diffusion of Na−22 into Corning Code 1737 glass

wet air, 1 atm
T = 650 °C
t = 183,960 s

Na Diffusion in Type I Silica Glass I

- **type A profiles are observed in Na-22 diffusion experiments in common and wet air at lower temperatures with as-received samples of Infrasil 302**

- **if the samples are pre-annealed at higher temperatures (900 - 1100 °C) in common or wet air, kinks are observed in tracer diffusion profiles generated at much lower temperature (650 °C), i.e., type C profiles are obtained**

- **the location of the kink, ℓ, as a function of the pre-annealing time follows a parabolic rate law**

diffusion of Na−22
as−received SiO_2
common air
T = 650 °C
t = 13,500 s

pre−annealed
in common air
T_{p-a} = 1000 °C
t_{p-a} = 132.7 h

t_{diff} = 9,900 s

diffusion of Na−22
into Type I silica glass

Comparison of Bulk Diffusion Coefficients

- **a comparison of sodium tracer diffusion coefficients obtained from Type A profiles is shown at the right**

- **sodium diffusion occurs in Type I silica glass much faster than in Corning Code 1737 glass**

- **a simple Arrhenius-type temperature dependence is found the diffusion of Na-22 in Type I silica glass (Infrasil 302); E_a = 101.8 $\pm$ 2.7 kJ/mol**

- **change in temperature dependence of the diffusion of Na-22 in 1737 glass at the strain point of this glass; two Arrhenius expressions needed to describe the temperature dependence of the sodium diffusion**
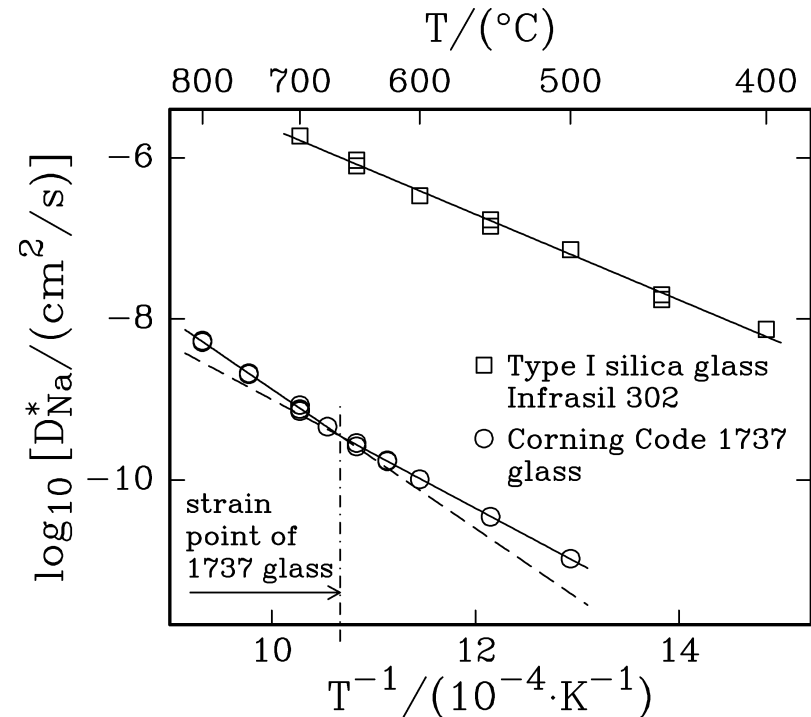
- **activation energies for Na diffusion in 1737 glass:**
  - **high T: 165.5 ± 3.0 kJ/mol**
 - **low T: 129.9 ± 1.2 kJ/mol**

Kink Displacement in Na Diffusion Profiles in Corning Code 1737 Glass Obtained After Diffusion-Annealing in Wet Air

- **discussed before that the integral water uptake of 1737 glass during annealing in wet air follows a parabolic rate law, i.e., that it is diffusion-controlled**

- **E_a = 139.4 ($\pm$ 34.4) kJ/mol for the water uptake; is related to the diffusion of H_2O**

- **kink displacement observed in diffusion profiles after diffusion-annealing in wet air follows also a parabolic rate law**

- **E_a = 195.6 ($\pm$ 5.2) kJ/mol for the kink displacement**

- **the difference between the two activation energies must be related to structural changes occurring upon the incorporation of water**

displacement of kinks in residual radioactivity profiles of Na−22 diffusing into Corning Code 1737 glass
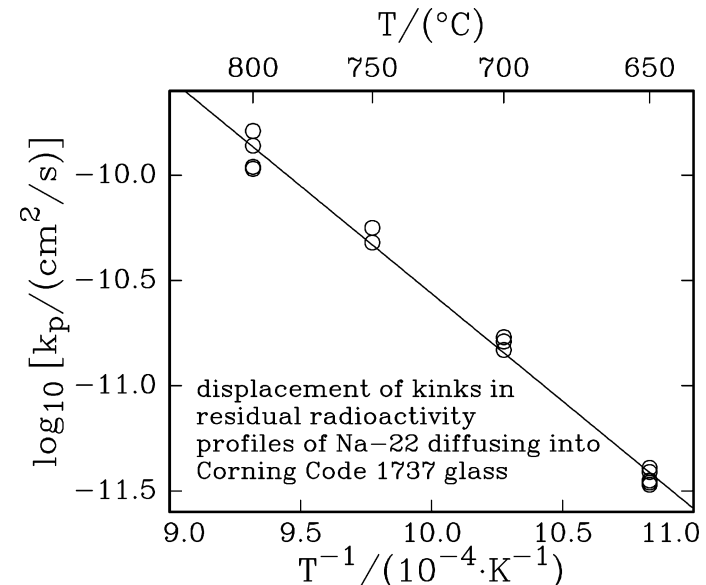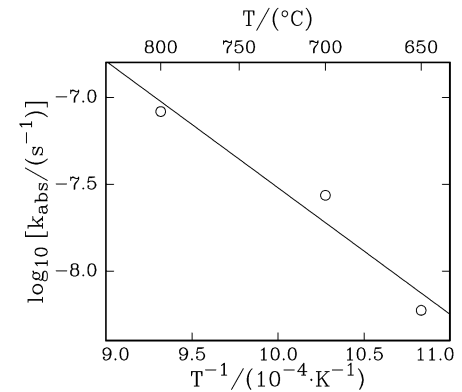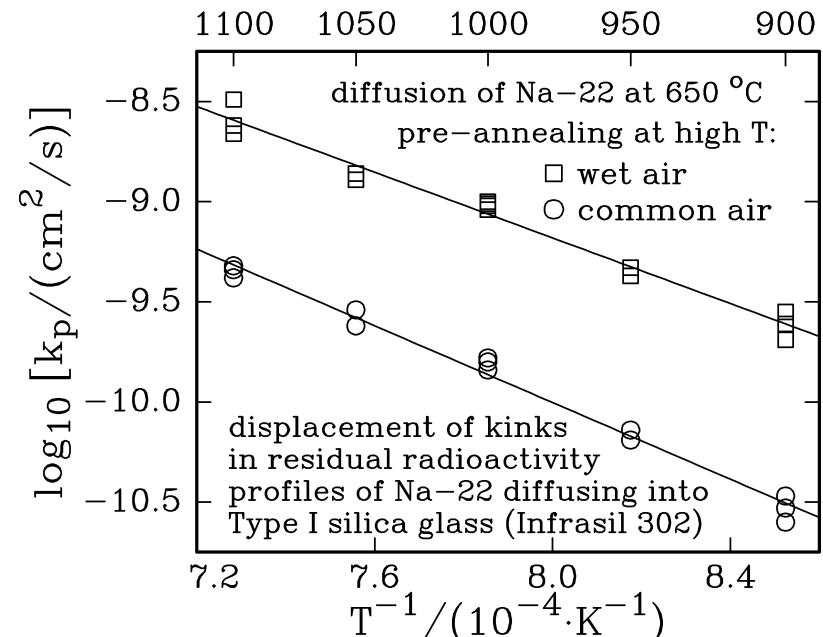
Comparison Between the Diffusion Rate of Na in the Near-Surface Region and in the Bulk of 1737 Glass

- **reduction of the Na+ diffusion rate near the surface due to the uptake of water**

- **D_{Na}(ns) 100 to 1000 times smaller than D_{Na}(bu) (ns = near the surface, bu = bulk)**

- **only little scatter in the ratio D_{Na}(ns)/D_{Na}(bu)**

- **no time dependence of the ratio D_{Na}(ns)/D_{Na}(bu), i.e., structural changes upon the uptake of water must occur relatively fast**
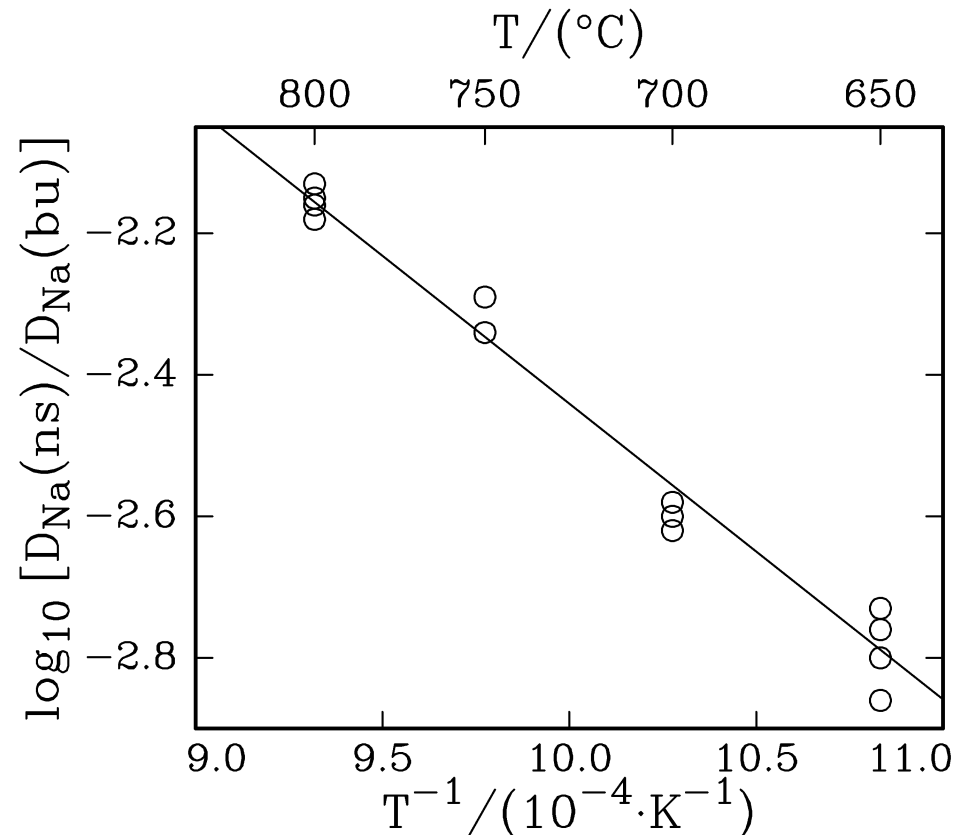
- **occurrence of kinks can be linked to an uptake of water by the silica glass (Infrasil 302) during pre-annealing**

- **water uptake at high temperatures can be described by a parabolic rate law**

- **as stated before, the location of the kink in type C profiles changes with the pre-annealing time following a parabolic rate law, see the figure at the right**

- **activation energies for kink displacements:**
  - **in wet air: 156.9 $\pm$ 7.0 kJ/mol**
  - **in common air: 183.4 $\pm$ 6.3 kJ/mol**
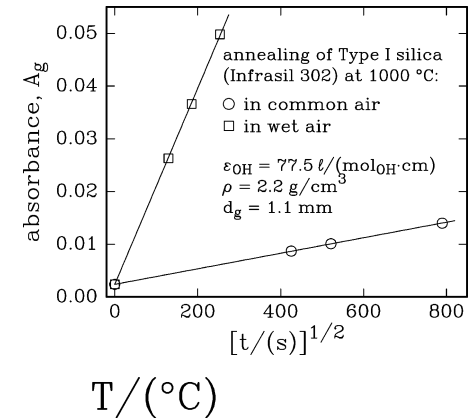
annealing of Type I silica (Infrasil 302) at 1000 °C:
○ in common air
□ in wet air

$\varepsilon_{OH} = 77.5 \ \ell/(mol_{OH}\cdot cm)$
$\rho = 2.2 \ g/cm^3$
$d_g = 1.1 \ mm$

diffusion of Na−22 at 650 ^{o}C
pre−annealing at high T:
□ wet air
○ common air

displacement of kinks in residual radioactivity profiles of Na−22 diffusing into Type I silica glass (Infrasil 302)

- **conclusions:**
  - **water is responsible for changes in sodium tracer diffusion coefficients near the surface**
  - **following ideas by Tomozawa, a structural relaxation occurs upon the incorporation of water into silica glass, leading to changes of structure-sensitive properties, including the diffusion of Na**

- **activation energy for the diffusion of water in silica 76 kJ/mol, i.e., much smaller than that observed for the kink displacement**

- **activation energy differences to be attributed to structural relaxation processes occurring upon the incorporation of water**

- **good agreement with data obtained by Tomozawa for structural relaxation in the form of a relaxation diffusion coefficient, D**
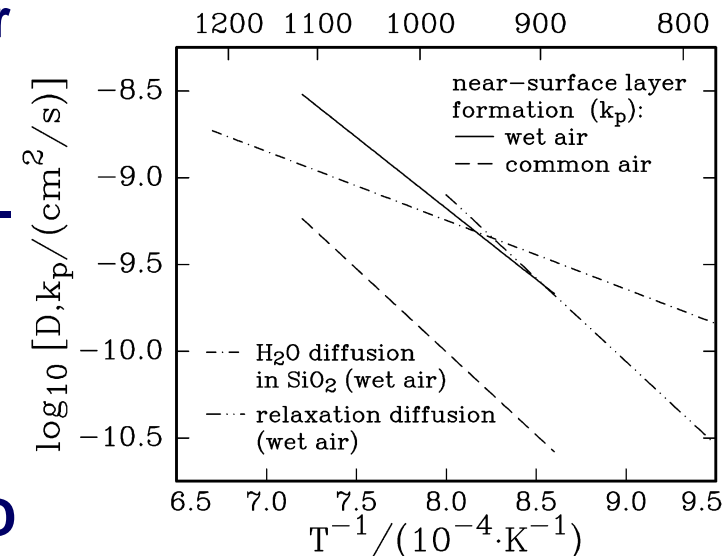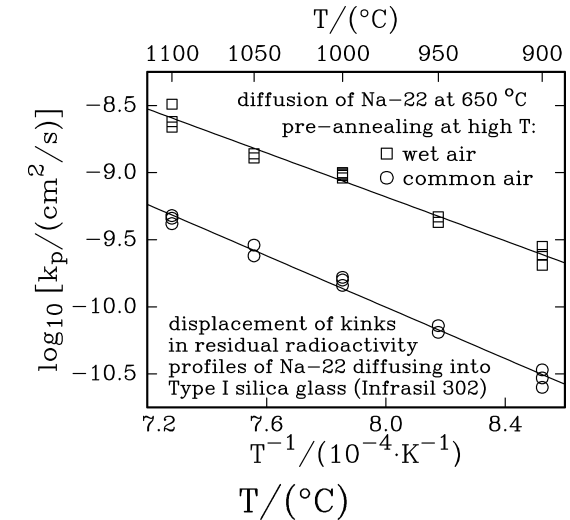
Comparison Between the Diffusion Rate of Na in the Near-Surface Region and in the Bulk of Type I Silica Glass

- $D_{Na}(ns)/D_{Na}(bu)$ about 1/300 to 1/100
- values for the ratio $D_{Na}(ns)/D_{Na}(bu)$ scatter very strongly
- the amount of water incorporated seems not to have any significant influence
- surprise when plotting the ratios obtained for different pre-annealing temperatures as a function of the pre-annealing time: the ratio seems to increase as a function of the annealing time
- reasons behind not yet understood; may be related to different processes involved in structural changes occurring upon the uptake of water during pre-annealing
- need additional data for shorter and longer pre-annealing times
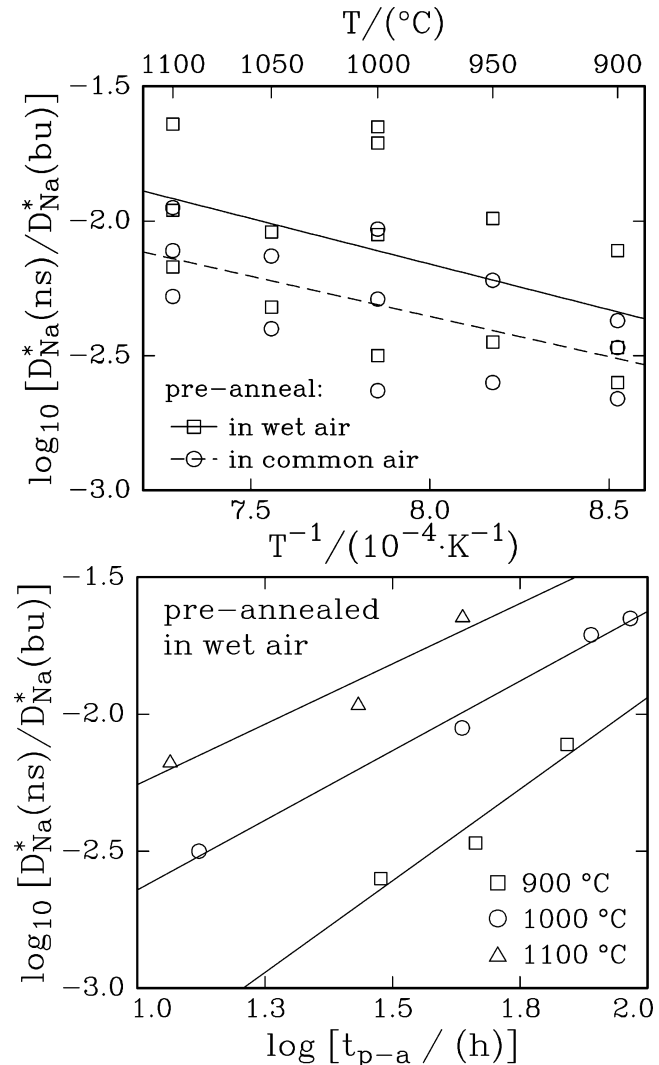
Mechanism of the Diffusion of Na in Infrasil 302 Type I Silica Glass

- **majority impurity: Al (about 30 ppma); expected to be located to a very large extent on Si sites**

- **Na present at a level of 1 ppma**

- **estimate on the spacing between Al in $[AlO_4]^-$ groups (= "traps") assuming a uniform distribution: 26 nm**

- **trapping of Na^+ at $[AlO_4]^-$ groups, which carry a negative excess charge, expected**

- **migration of Na^+ then from trap to trap through "interstitial sites" in silica glass at a very high rate**

$[AlO_4]^-$ silica $[AlO_4]^-$
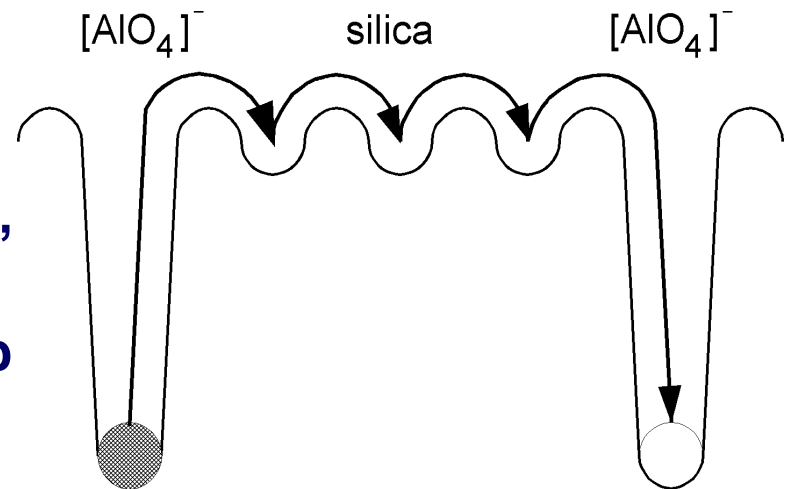
Structural Relaxation in Type I Silica Glass

- **the reduction in the sodium diffusivity in near-surface region after pre-annealing in moist atmospheres is attributed to a structural relaxation**

- **reaction between water incorporated into glass**

  $$R-O-R' + H_2O \Leftrightarrow R-O-H + R'-O-H$$

- **equilibrium is dynamic and allows for a "water-assisted" relaxation processes**

- **to explain the observed time-dependence of $D_{Na}(ns)/D_{Na}(bu)$ two relaxation processes must be present; speculation:**

  - **fast relaxation around $[AlO_4]^-$ units, leading to a very significant reduction of $D_{Na}(ns)/D_{Na}(bu)$**

  - **slow relaxation in the rest of the glass, leading to an increase of $D_{Na}(ns)/D_{Na}(bu)$**

assumed for calculation:
$\tau_1 = 0.1$ h
$\tau_2 = 100$ h
1: decrease by 1000
2: increase by 10
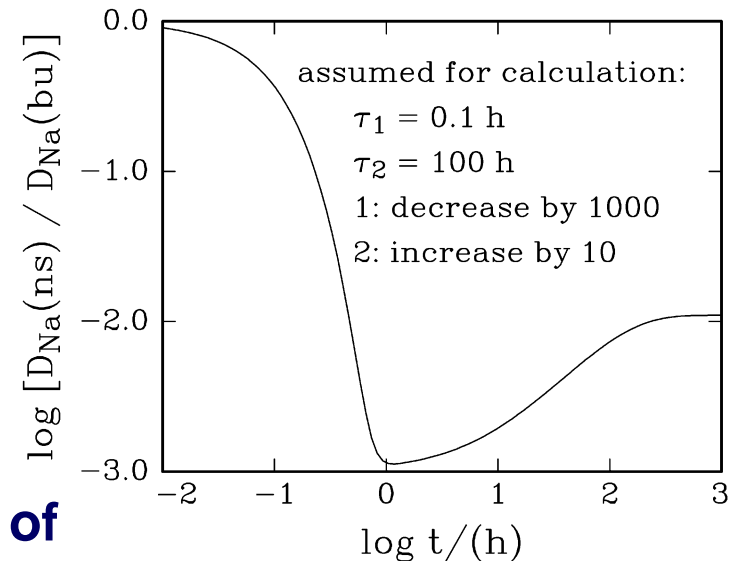
Characterization of the Effectiveness of Diffusion Barrier Layers

- sandwich of two samples with a "barrier layer" between them used
- first: generation of a tracer diffusion profile in Sample 1 by diffusion annealing at high temperature
- then generation of a "barrier layer" at the surface of Sample 2, e.g., by deposition, annealing in wet air, etc.
- then diffusion anneal of the sandwich, leading to a redistribution of the tracer
- after that, analysis of the resulting tracer distribution, e.g., by measuring a residual radioactivity profile
- diffusion mathematics needed for the data analysis worked out for different tracer distributions in Sample 1 before annealing the sandwich; the math is relatively complex
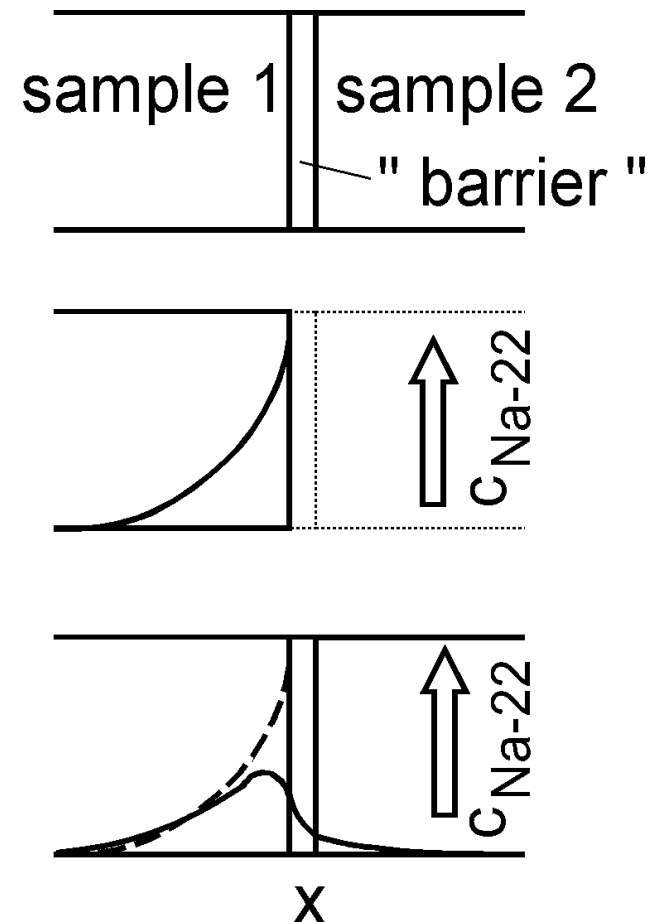
Principles of Diffusion Mathematics

- **equations governing the diffusion in Sample 1 and in Sample 2**

$$\frac{\partial c_1}{\partial t} = D_1^* \cdot \frac{\partial^2 c_1}{\partial x^2} \quad x < 0 \quad \text{and} \quad \frac{\partial c_2}{\partial t} = D_2^* \cdot \frac{\partial^2 c_2}{\partial x^2} \quad x > 0$$

- **regions x > 0 and x < 0 connected by the condition of continuity of flux at x = 0, i.e.,**

$$D_1^* \cdot \left.\frac{\partial c_1}{\partial x}\right|_{x=0^-} = D_2^* \cdot \left.\frac{\partial c_2}{\partial x}\right|_{x=0^+} = -k_i \cdot \left(\left.c_1\right|_{x=0^-} - \left.c_2\right|_{x=0^+}\right)$$

- **k_i is a rate constant for the transfer of the diffusing species across the "barrier layer"**

- **diffusion equations to be solved taking into account the initial tracer distribution in Sample 1, g(x), e.g., given by the thin film solution of Fick's second law, i.e.,**

$$g(x) = c_1(x < 0, t = 0) = \frac{q}{\sqrt{\pi \cdot D_1^* \cdot t_0}} \cdot \exp\left(-\frac{x^2}{4 D_1^* \cdot t_0}\right)$$

- **t_0 is the diffusion time of the first anneal with Sample 1 only**

Equations for Concentration Profile

- **equation for the concentration in Sample 1 ($x < 0$) as a function of x and t:**

$$c_1(x,t) = \frac{q}{\sqrt{\pi \cdot D_1^* \cdot (t + t_0)}} \cdot \exp\left(-\frac{x^2}{4D_1^* \cdot (t + t_0)}\right) + \int_0^t \frac{\exp\left(-\frac{x^2}{4D_1^* \cdot (t - \tau)}\right)}{\sqrt{\pi \cdot D_1^* \cdot (t - \tau)}} \cdot \varphi(\tau) \cdot d\tau$$

- **equation for the concentration in Sample 2 ($x > 0$) as a function of x and t:**

$$c_2(x,t) = -\int_0^t \frac{\exp\left(-\frac{x^2}{4D_2^* \cdot (t - \tau)}\right)}{\sqrt{\pi \cdot D_2^* \cdot (t - \tau)}} \cdot \varphi(\tau) \cdot d\tau$$

- **equation for the function $\varphi(\tau)$:**

$$\varphi(\tau) = \frac{k_i \cdot q}{\sqrt{D_1^*}} \cdot \left[\begin{array}{l} -\frac{1}{\sqrt{t + t_0}} + 2\left(1 + \sqrt{\frac{D_1^*}{D_2^*}}\right) \cdot \frac{k_i}{\sqrt{\pi \cdot D_1^*}} \cdot \sin^{-1}\sqrt{\frac{t}{t + t_0}} \\[2em] -\left(1 + \sqrt{\frac{D_1^*}{D_2^*}}\right)^2 \cdot \frac{k_i^2 \cdot \sqrt{t_0}}{D_1^*} \cdot \int_0^{t/t_0} \frac{1}{\sqrt{1 + T'}} \cdot \exp\left\{\left(1 + \sqrt{\frac{D_1^*}{D_2^*}}\right)^2 \cdot \frac{k_i^2 \cdot t_0}{D_1^*} \cdot \left(\frac{t}{t_0} - T'\right)\right\} \\[2em] \cdot \mathrm{erfc}\left\{\left(1 + \sqrt{\frac{D_1^*}{D_2^*}}\right) \cdot k_i \cdot \sqrt{\frac{t_0}{D_1^*} \cdot \left(\frac{t}{t_0} - T'\right)}\right\} \cdot dT' \end{array}\right]$$

- **numerical solution of integrals of theses functions used for calculating residual radioactivity profiles and also for data fitting**

Concentration and Residual Radioactivity Profiles

- **profiles calculated for $D_1 = D_2 = 10^{-10}$ cm^2/s and different values of k_i**

- **t_0 = 90,000 s, t = 90,000 s**

- **top figure: initial profile after diffusion anneal of Sample 1 only and profiles after annealing sandwiches**

- **bottom figure: residual radioactivity profiles corresponding to the concentration profiles shown in the top figure**

- **experiments: measured residual radioactivities and derived data for k_i and for $D_1 = D_2$ from fits**

- **values of k_i give information on the efficiency of a barrier**
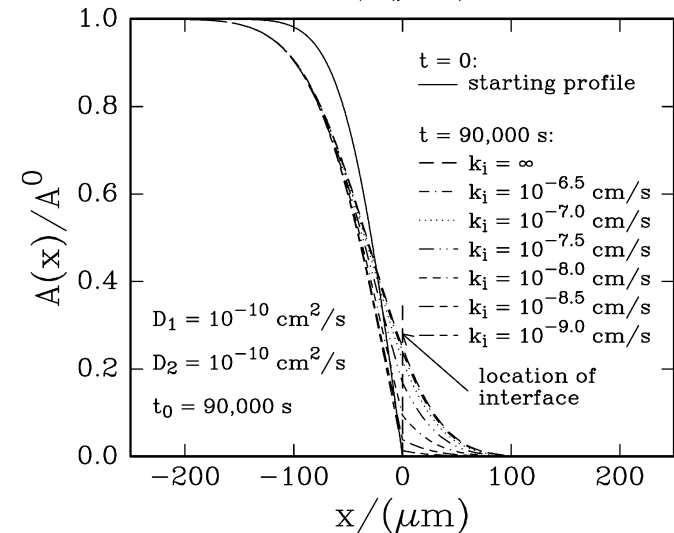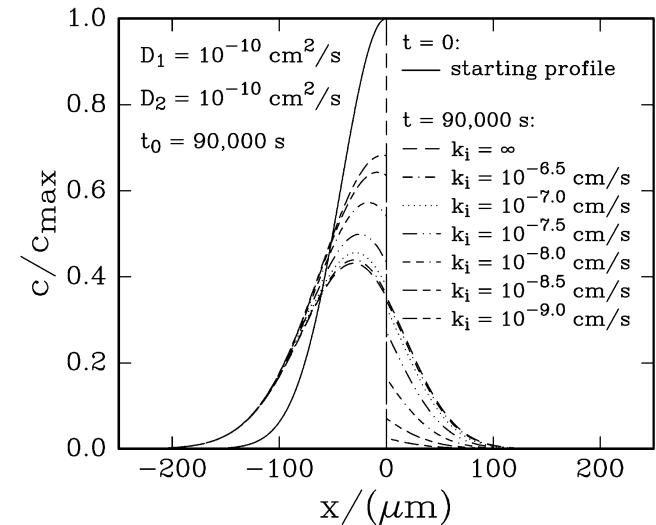
Experimental Observations 23.6 h

- **annealing of Sample 1 at 650 °C in common air for about 1 day for generating the initial tracer concentration profile**

- **annealing of Sample 2 in wet air for 23.6 hours in wet air for modification of the near-surface layer**

- **then diffusion anneal of sandwich for about 1 day**

- **top figure: overall residual radioactivity profile**

- **bottom figure: magnified part of the same figure in the region x > 0**

- **solid lines: from fit of the equation discussed before to the experimental data**

Top figure annotations:
$D_{Na}^{*} = 2.69 \cdot 10^{-10}\ cm^2/s$
$t_0 = 95{,}800\ s$
$t = 89{,}300\ s$
$T = 650\ °C$

- – – ideal contact, i.e., $k_i = \infty$
- —— from fit
- ○ barrier: generated by 23.6 hours wet air annealing $k_i = 1.77 \cdot 10^{-9}\ cm/s$

Axes: $A(x)/A^0$ vs $x/(\mu m)$

Bottom figure:
- – – ideal contact, i.e., $k_i = \infty$
- ○ barrier: generated by 23.6 hours wet air annealing $k_i = 1.77 \cdot 10^{-9}\ cm/s$
- —— from fit

Axes: $A(x)/A^0$ vs $x/(\mu m)$
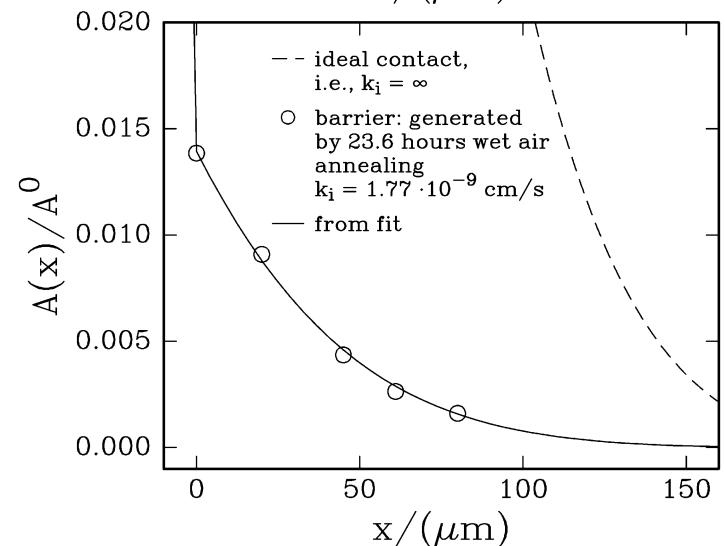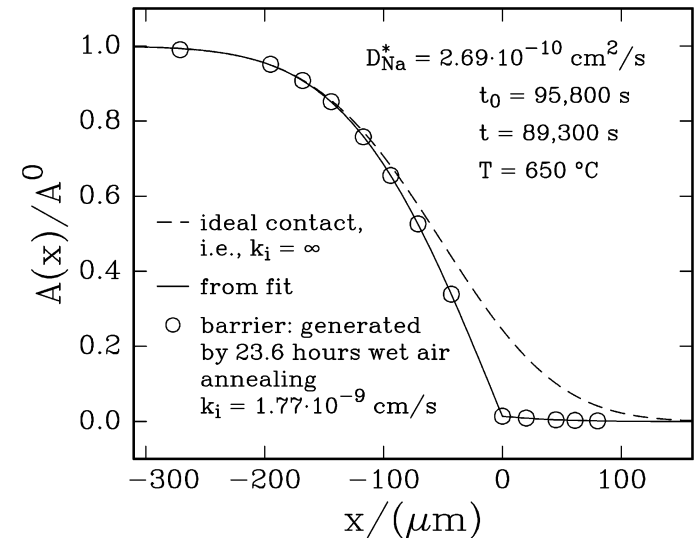
Experimental Observations II

- **experiments performed with four different times for the water incorporation times into Sample 2**

- **Na-diffusion coefficients very consistent**

water uptake time (h)	log [D_{Na}/(cm^2/s)]	log [k_i/(cm/s)]
11.4	−9.527 ± 0.004	−8.568 ± 0.097
23.6	−9.571 ± 0.001	−8.752 ± 0.033
50.2	−9.564 ± 0.001	−8.907 ± 0.085
86.3	−9.484 ± 0.003	−9.094 ± 0.228

- **values for D_{Na} in very good agreement with results from separate tracer diffusion experiments at 650 °C**

- **values for k_i decrease with increasing water uptake time, corresponding to an increasing barrier layer thickness**

- **also experiments with SiO_2 CVD films as barrier layers and with (very ineffective) barrier layers generated by RCA-cleaning**

Analysis of the Pre-Annealing Time Dependence of k_i

- **average sodium tracer diffusion coefficient in the barrier layer, D_{bar}:**

$$D_{bar} = k_i \cdot d_{bar}$$

d_{bar} = barrier thickness, k_i = rate constant for transfer of Na across the barrier

- **flux of Na across barrier layer:**

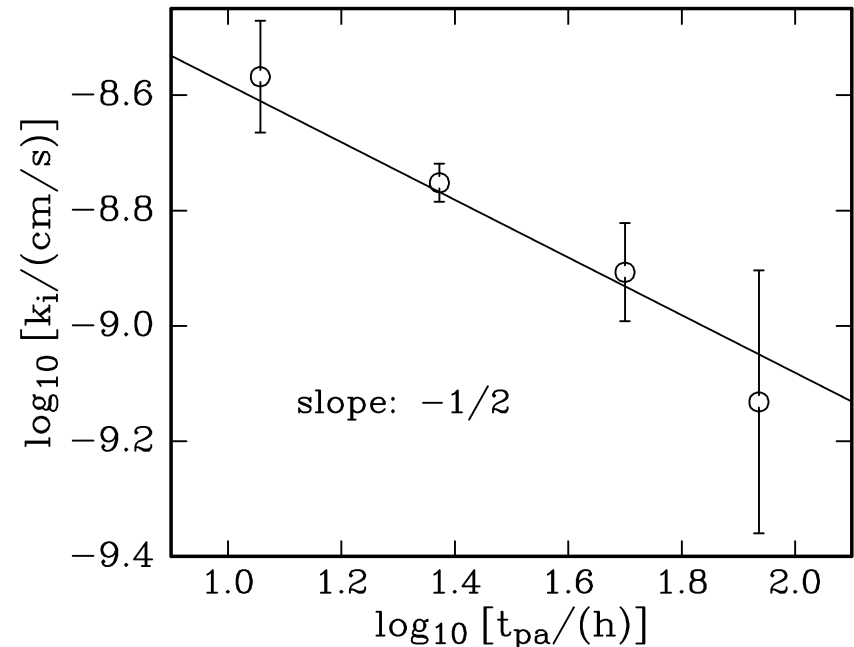$$j_{Na} = k_i \cdot \Delta c_{Na} = D_{bar} \cdot \frac{\Delta c_{Na}}{d_{bar}}$$

- **thickness of barrier layer:**

$$d_{bar} = \sqrt{k_p \cdot t_{pa}}$$

k_p = parabolic rate constant for the near-surface layer generation

- **relation between k_i and the pre-annealing time, t_{pa}:**

$$k_i = \frac{D_{bar}}{\sqrt{k_p}} \cdot t_{pa}^{-1/2}$$

slope: $-1/2$

values determined experimentally for k_i are by a factor of about 2 larger than values predicted for k_i by using values for k_p and for D_{Na} from separate experiments - it is unknown why this is so

CONCLUSIONS

- **silicate glasses (e.g., Infrasil 302 and Corning Code 1737 glass) may take up water from the environment during high temperature annealing in air containing some water, i.e., they are "thirsty"**

- **the water uptake follows a parabolic rate law, i.e., it is to a large extent diffusion controlled**

- **water-assisted structural changes are believed to occur as a result of the water uptake**
  - **leads to a modification of glass properties near the surface**
  - **causes a decrease in the mobility of sodium ions in the near-surface region**

- **opens the possibility to make "functionally graded" glass**

- **example: generation of a sodium diffusion barrier layer on Corning Code 1737 glass**

ACKNOWLEDEMENTS

- **diffusion work**
  - **Hongxia Lu, Lei Tian (graduate students)**
  - **Eric Chalfin, Eric Hoke, Timothy Lau, Rojana Pornprasertsuk, Marissa Sweeney (undergraduates)**

- **IR-studies**
  - **Greg Couillard (Corning Inc.)**
  - **Hongxia Lu (graduate student)**

- **diffusion mathematitics:**
  - **Chung-Yuen Hui, Michael O. Thompson (Cornell faculty)**
  - **Yu-Yun Lin (graduate student)**

- **glass samples**
  - **Adam Ellison (Corning Inc.)**

- **funding:**
  - **NSF via the Cornell Center for Materials Research (CCMR)**